Adaptive control for a lightweight robotic arm actuated by a shape memory allow wire.

QUINTANAR-GUZMAN, S., KANNAN, S., VOOS, H., DAROUACH, M. and ALMA, M.

2018

Adaptive control for a lightweight robotic arm actuated by a Shape Memory Allow wire

S. Quintanar-Guzmán[1], S. Kannan[1], H. Voos[1], M. Darouach[2], M. Alma[2]

[1]University of Luxembourg, Luxembourg, Grand Duchy of Luxembourg.

[2]University of Lorraine, Longwy, France.

Abstract:

This paper presents the design, model and closed-loop control of a single degree-of-freedom (DOF) lightweight robotic arm actuated by a biased Shape Memory Alloy (SMA) wire. The highly non-linear dynamics of SMAs represent a challenge for control tasks, due to phenomena as hysteresis or parameters uncertainty. With this in mind, we propose a control capable to adapt itself to the hysteretic behavior and update its behavior to deal with the changing parameters of the material over time. An adaptive control for position regulation is presented. This control includes a set of techniques, providing a systematic way to adjust the control parameters in real time, so maintaining the stability of the system and a desired performance, while dealing with parameter and model uncertainties. The closed-loop approach is tested in experimentally showing its effectiveness to deal with the highly non-linear dynamics of the SMA wire.

Keywords: SMA wire, adaptive control, lightweight, robotic arm

Introduction

Shape Memory Alloys (SMA) are a type of the so called "intelligent materials". They are capable of recovering their original shape after being deformed, when submitted to controlled thermal or mechanical stimuli. This recovery effect is known as Shape Memory Effect (SME). This effect happens due to an internal transformation on the microstructures of the material. When the material is at lower temperature it shifts to a phase called martensite, which is highly malleable structure, thus the material can be deformed. When the material is heated it shifts back to an austenitic phase recovering its original shape [1].

These intelligent materials present multiple advantages over traditional actuators, such as high force to mass ratio, noiseless operation, biocompatibility, corrosion resistance, among others. These characteristics make them suitable for a wide range of application substituting traditional actuators as DC motors or hydraulic effectors [2]. Applications such as orthopedic devices [3], dental applications [4], aerodynamic applications as morphing wing segments [5, 6]. Other implementation such as actuator for human-like robotic arms [7] or finger prosthetics [8].

However, most of the engineering application where these material are implemented as actuators require complicated and heavy mechanisms or micro-scale working environments. To solve this inconvenient, a lightweight SMA actuated robotic arm, based on 3D printed pieces with simple mechanisms and light constructions materials was presented in a previous publication [9]. The present article propose mechanical improvements to this design and a complete new design for the end-effector, improving the overall performance of the mechanism.

In spite of all the advantages SMA have, they also present some challenges when used in applications that require high precision control. These materials have a highly nonlinear hysteretic behavior and multiple other nonlinear phenomena in their dynamics like dead zone, super-elasticity or shifting parameters. To deal with these nonlinear dynamic, multiple control approaches have been developed. In [10] a comparative study among 4 different types of controllers was performed, being the adaptive control the approach with better results. Different adaptive controllers have been developed for controlling SMA wires. For example in [11, 12] a direct linear adaptive control for a single SMA wire actuated robotic arm was proposed. While in [13] an indirect adaptive predictive control was used. Also intelligent adaptive methods using neural networks [14] or adaptive fuzzy control [15].

The present work contains two main contributions: first an improved design of a lightweight robotic arm is presented, were the use of any traditional actuator is avoided by the implementation of a couple of SMA wires to control the position of the end-effector and

actuation of the gripper. Second, a previously proposed direct adaptive control is tested experimentally and compared with a traditional control approach.

The remaining of this article is organized as follow. First the mechanical design of the SMA actuated robotic arm is presented, followed by the mathematical model of the full system. After, the adaptive control approach is developed, followed by the design of a PID control for comparative means. Subsequently the experimental setup is presented and the experimental results discussed. Finally, we conclude with final comments and future work.

SMA actuated Robot arm design

The mechanical design of the lightweight SMA actuated robotic arm is presented in this section. In Fig. 1 a computer aided design (CAD) model of the proposed robotic arm is presented. This design is based on a previously published work [10], with several improvements on the general mechanical design and mainly on the end-effector's design.

The robotic arm is a one Degree-of-freedom (DOF) lightweight SMA actuated system. This consists of two couplers joint by a torsion spring. Coupler-1 is actuated by a SMA wire while the Coupler-2 is fixed with a hard wire (Wire-2), giving a single SMA wire actuator configuration with the torsion spring as the bias force. The end-effector is attached to the Coupler-1 and it is actuated by a second biased SMA wire. The bias force for the end-effector's actuation is generated by a 3D-printed custom-designed spring. This spring allows to convert the transversal movement of the second SMA wire into longitudinal movement along the end-effector's shaft, generating the open-close motion of the gripper.

The mechanism is mostly 3D printed with exception of the shafts and groove bearings. The shafts of the design are carbon fiber custom-made to increase the stiffness and keep the low weight. On the other hand, due to thermal problems with 3D printed parts, the groove bearings are metallic pieces that allow to accommodate the necessary length of the SMA wire to achieve the desired displacement without increase the overall size of the robotic arm.

The use of SMA wires as actuators, together with a simple mechanical design and lightweight construction materials, allow for the construction of a robotic arm with an approximate weight of 50g and rotational movement span of the end-effector of 70 degrees. The lightweight design, together with its wide range of rotation capability, makes of this design a suitable alternative for aerial manipulation with small unmanned aerial vehicles (UAVs).

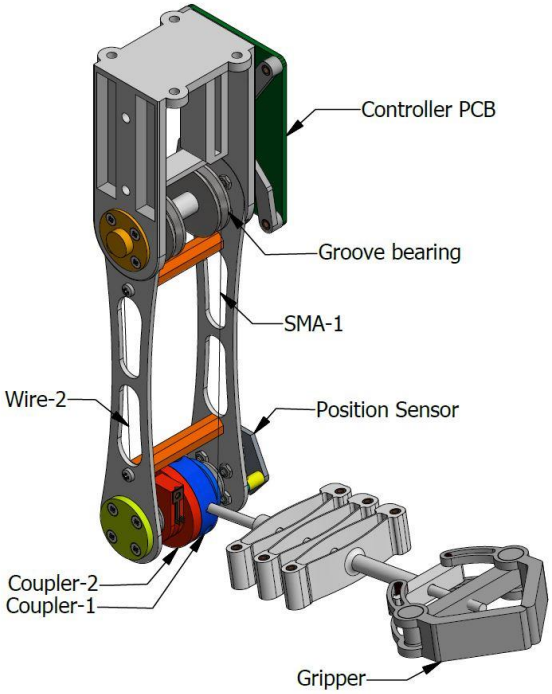

Fig. 1: *SMA actuated robot arm CAD model.*

System model

In this section the mathematical model of the proposed robotic arm will be presented. The overall model consist of three subsystems as shown in Fig. 2 the three submodels conforming the robotic arm's mathematical model are 1) SMA wire model, 2) Kinematic model and 3) Dynamic model.

SMA wire model. This model describes the dynamics of the SMA wire under thermal and mechanical stimuli. This model is further divided by three submodels as shown in Fig**. 3**, which interaction generates a recursive model. First the Heat Transfer model outlines the thermal effect of the control voltage over the SMA wire by Joule effect and natural convection, where the latter is approximated by a second order polynomial of the temperature.

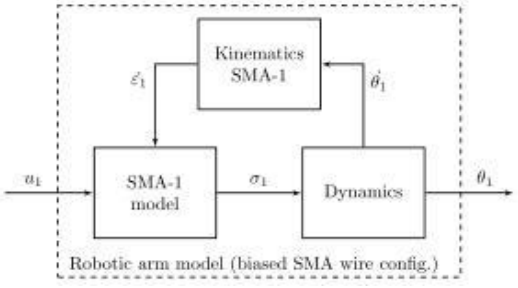

Fig. 2: *SMA actuated robotic arm model block diagram.*

The Phase Transformation Model computes the martensite fraction rate of the SMA wire ($\dot{\xi}$). This model consist of a set of two dynamic equations describing the cooling and heating behaviour of the system respectively. These two equations are necessary to represent the characteristic hysteresis of the SMA wire's dynamic. The martensite fraction depends on the temperature and stress of the SMA wire, being a highly nonlinear model.

The constitutive model characterizes the interaction between the SMA wire's dynamic states and the mechanical effects of these states over the overall actuator. This effect is describe by the stress rate ($\dot{\sigma}$) as follows [16, 17]:

$$\dot{\sigma} = E\dot{\varepsilon} + \Omega\dot{\xi} + \Theta\dot{T} \qquad (1)$$

where the model describes the relation among the strain rate ($\dot{\varepsilon}$), martensite fraction rate ($\dot{\xi}$) and temperature derivate ($\dot{T}$).

Kinematic model. This model depicts the interaction between the SMA model and dynamics of the arm. The kinematic model depends directly on the mechanical design, since it relates directly to the geometry of the actuator.

Dynamic model. The general dynamic equation of the proposed robotic arm is given by:

$$I_M(\theta)\,\ddot{\theta} + C_m\left(\theta,\dot{\theta}\right) + g(\theta) + V_d\dot{\theta} + \Phi(\theta,\theta_r) = \tau_\omega \qquad (2)$$

where θ and its time first and second derivate represent the position, velocity and acceleration of coupler-1, $I_M(\theta)$ is the inertia matrix and $C_m\left(\theta,\dot{\theta}\right)$ the centripetal-coriolis matrix. The effect of the gravity is considered in $g(\theta)$ and V_d represents the viscous coefficient term. $\Phi(\theta,\theta_r)$ represents the nonlinear hysteretic term and τ_ω is the input torque applied to the coupler-1 by the SMA wire. The latter can be mathematically described as:

$$\tau_\omega = F_\omega r = A\sigma r \qquad (3)$$

For a more detail description of the full SMA wire actuated robotic arm model, please refer to [10].

Position regulation adaptive control design

In this section the design of the adaptive control for position regulation of the robotic arm's end-effector is presented.

The robotic arm is controlled via voltage signals applied to each individual SMA wire. The gripper is controlled by an On-Off control where the only states possible are open and closed. On the other hand, the robotic arm should be capable to position the end-effector in any angle within the allowed range of movement.

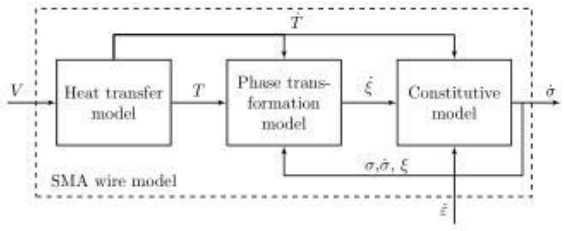

Fig. 3: *Shape Memory Alloy model block diagram.*

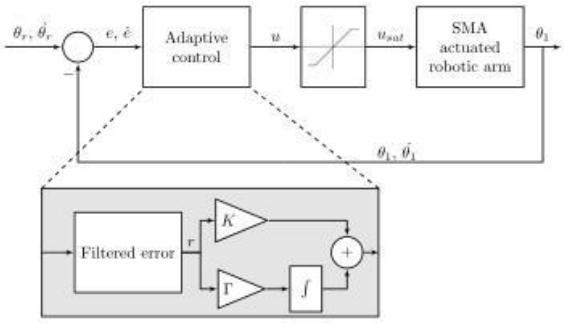

Fig. 4: *Adaptive Control block diagram.*

For this end, an adaptive control law based on the system's mathematical model is developed.

In **Fig. 4** a block diagram of the closed-loop system is shown. Here a direct adaptive control method is applied for position control together with a saturation block to restrict negative voltages and avoid overheating of the SMA wire, which could cause damage to the memory effect.

Let us define the angular position error (e) as

$$e = \theta_r - \theta \qquad (4)$$

where θ_r is the desired joint angle position. We defined the first time derivative of the error as

$$\dot{e} = \frac{d}{dt}e \qquad (5)$$

The filtered position error is written as [18]

$$r(t) = \dot{e}(t) + \alpha e(t) \qquad (6)$$

where α is a positive known constant. After algebraic manipulation, the open loop dynamics of the systems can be written in terms of the filtered error (r) as [18]

$$I_M(\theta)\dot{r} = -C_m\left(\theta,\dot{\theta}\right)r + \varsigma - \tau \qquad (7)$$

and

$$\varsigma = I_M(\theta)\left(\ddot{\theta}_r + \alpha\dot{e}\right) + C_m\left(\theta,\dot{\theta}\right)\left(\dot{\theta}_r + \alpha e\right) + g(\theta) + V_d\dot{\theta} + \Phi(\theta,\theta_r) \qquad (8)$$

Choosing the control input based on (7)

$$\tau = \hat{\varsigma} + Kr \qquad (9)$$

where K is the control gain and $\hat{\varsigma}$ is the estimate of ς. And the estimate is updated by

$$\hat{\varsigma} = \Gamma^{-1} r \qquad (10)$$

being Γ a positive definite adaptation gain. Substituting (7) $I_M(\theta)\dot{r} = -C_m(\theta, \dot{\theta})r + \varsigma - \tau$ *(7)* in (9)$\tau = \hat{\varsigma} + Kr$ *(9)* we can written the closed loop system dynamics in terms of r as:

$$I_M(\theta)\dot{r} = -C_m(\theta, \dot{\theta})r + Kr + \tilde{\varsigma} \quad (11)$$

where $\tilde{\varsigma} = \varsigma - \hat{\varsigma}$. For further details on the control development and the stability analysis please refer to [12, 11].

PID position control design

For the purpose of performance comparison, a PID control is designed. This control approach is one of the simplest for angular position regulation on robotic systems.

Considering the angular position error defined in (4) the PID control law is given by:

$$u(t) = K_p e(t) + K_i \int e(t)\, dt + K_d \dot{e}(t) \qquad (12)$$

where K_p, K_i and K_d are the proportional, integral and derivative gains respectively.

Experimental results

In the following section the experimental results of the proposed adaptive control (AC) and PID control are compared and discussed.

The experimental setup is shown in **Fig. 6**. Matlab/Simulink on a computer controls the position of the robotic arm using a voltage power supply through a power interface based on MOSFET PMV16XN. The voltage signal is delivered using PWM control. The position of the end-effector is measured by a potentiometer Bourne 3382G along with a 12 bits ADC. The communication between Matlab/Simulink and the actuator is via serial port with a microcontroller ESP-12E as interface. The sampling time was set to 10 ms. Although the communication for this test is wired, the robotic arm is equipped and designed for wireless communication through Robot Operating System (ROS).

A 0.31 mm diameter and 40 cm length Flexinol® SMA wire is used for SMA-1. The gripper is actuated by a 0.15 mm diameter and 10 cm length Flexinol® SMA wire. The arm's couplers have a diameter of 7.5 mm and are joined by a spring with a stiffness constant of 3.2 Nmm per degree.

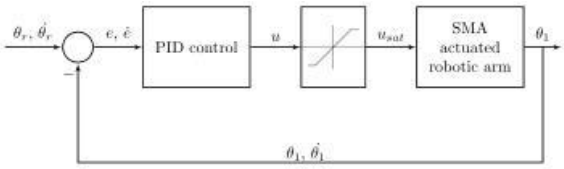

Fig. 5: *PID Control block diagram.*

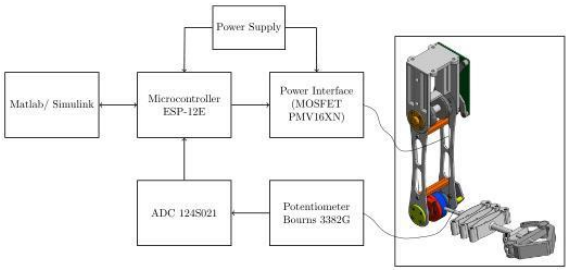

Fig. 6: *Experimental setup.*

Both controllers were tuned heuristically, due to the highly nonlinear dynamics inherent to SMA wires. The gains for the AC control were set as $\alpha = 2$ and $K = -0.4$. In addition, the gains for the PID control were $K_p = -0.3$, $K_i = -0.06$ and $K_d = -0.01$. The control signal for both controller is limited by a saturation block in order to avoid high voltages that could cause overheating and damage to the SMA wire. The upper limit for both controllers is set to 5 V. At the same time the saturation block sets the lower voltage limit to 0 V, since negative voltages are not capable of generating a cooling effect on the system.

The performance of the proposed adaptive control is tested for position regulation with a series of 3 steps at 0, 20 and 40 seconds time respectively (see **Fig. 7** dashed line). The results are then compared with the PID control under similar conditions. A 5 seconds lapse is given at the beginning of the data acquisition before the control action is started. The initial position of the robotic arm is the equilibrium point with SMA-1 at maximum strain ($\approx 62°$). The angular position is measured as the rotational position of the end-effector with respect to the horizontal plane.

Fig. 7 shows the comparison of the closed-loop performance of both AC and PID control. From this figure it is clear that the system has a better response during falling steps, where the SMA-1 is actuated. This is due to the free dynamic during cooling, when actuating with a biased configuration. The response of the system present an average overshoot of 4.5% with AC and 8.3% for PID control. The average steady-state error (SSE) is 0.23% for the AC while for PID control is 0.33%. In addition, the average settling time for falling steps is 3.25s for AC and 6.25s for PID control. As mentioned before, both controllers

have a poor performance during raising steps, where the settling time for both controller is on average 10s.

The AC controller have better overall results, decreasing the all three parameters, average overshoot, average steady-state error and settling time. However, both controllers had a poor performance when facing raising steps references, we can conclude that the AC approach is more suitable for dealing with the SMA wires nonlinear dynamics. This is better shown in **Fig. 8**, where the position regulation error is presented.

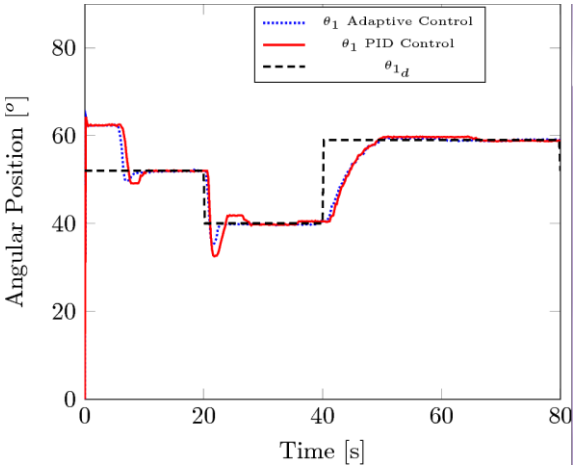

Fig. 7: *Comparison of PID and AC controllers for position regulation.*

The control input for both controllers is depict in **Fig. 9**. We can see that the adaptive control has a more aggressive response when compared to the PID control, however, it achieves faster responses and smaller SSE, while the control input is still between safe limits for the SMA wire.

Conclusions

We have presented a lightweight robotic arm actuated by a couple of biased SMA wires, one for gripper control and one for angular position control. This design in based on 3D printed custom-design pieces which along with light constructions materials allows a robotic arm with an approximate weight of 50g and a range of movement around 70 degrees.

A direct adaptive control (AC) for position regulation was developed. This controller was tested experimentally and its performance compared with a classical PID control, where the adaptive control proved to be a better approach to deal with the SMA wire nonlinear dynamic.

As future work the experimental results will be extended to two SMA wires configuration for joint actuation, looking to achieve with this approach a shorter settling time and smaller steady-state errors.

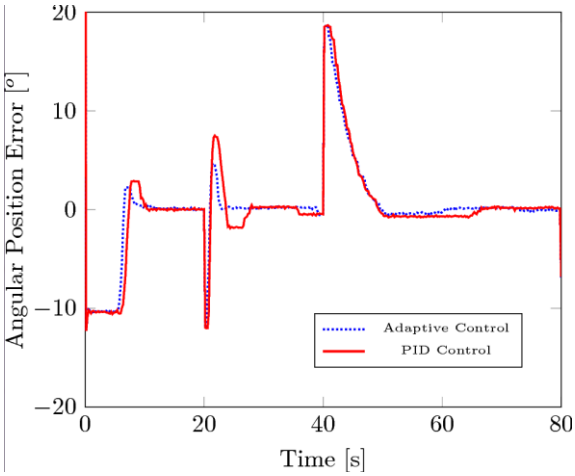

Fig. 8: *Regulation error for PID and AC controllers during position regulation.*

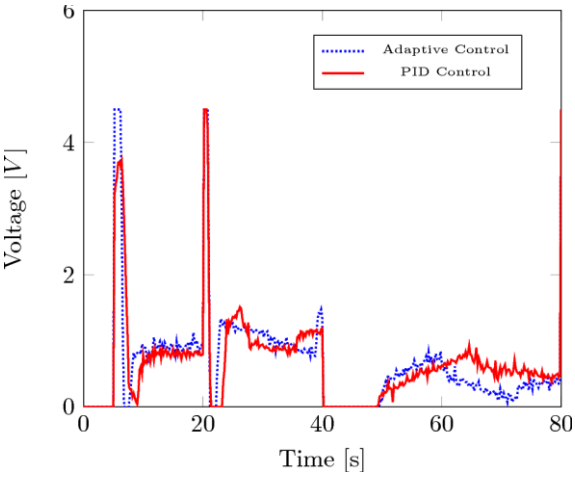

Fig. 9: *Control Voltage for position regulation with PID and AC controllers.*

References

[1] A. Rao, A. R. Srinivasa and J. N. Reddy, Design of Shape MEmory Alloyo (SMA) ACtuators, Berlin: Springer International Publishing, 2015.

[2] B. H. Shin, K. M. Lee and S. Y. Lee, "A miniaturized tadpole robot using an electromagnetic oscillatory actuator," *Journal of Bionic Engineering*, vol. 12, no. 1, pp. 29-36, 2015.

[3] M. T. Andani, W. Anderson and M. Elahinia, "Design, modeling and experimental evaluation of a minimally invasive cage for spinal fusion surgery utilizing superelastic

Nitinol hinges," *Journal of Intelligent Maetrial Systems and Structures*, vol. 26, no. 6, pp. 631-638, 2015.

[4] N. Pandis and C. P. Bourauel, "Nickel-titanium (NiTi) arch wires: the clinical significance of super elasticity," *Seminars in Orthodontics*, vol. 16, no. 4, pp. 249-257, 2010.

[5] H. Rodrigue, S. Cho and M. W. Han, "Effect of twist morphing wing segment on aerodynamic performance of UAV," *Journal of Mechanical Science and Technology*, vol. 30, no. 1, pp. 229-236, 2016.

[6] S. Barbarino, S. Ameduri and L. Lecce, "Wing shape control through an SMA-based device," *Journal of Intelligent Material Systems and Structures*, vol. 20, no. 3, pp. 283-296, 2009.

[7] M. Hulea and C. F. Caruntu, "Spiking neural network for controlling the artificial muscles of a humanoid robotic arm," in *Proceedings of the 2014 18th international conference on system theory, control and computing*, New York, 2014.

[8] L. v. d. E. Elst, S. Quintanar-Guzmán and J.-R. Hadji-Minaglou, "Design of an Electromechanical Prosthetic Finger using Shape Memory Alloy Wires," in *IEEE 5th International Symposium on Robotics and Intelligent Sensors*, Ottawa, Canada, 2017.

[9] S. Quintanar-Guzmán, S. Kannan, M. A. Olivares-Mendez and H. Voos, "Operational space control of a lightweight robotic arm actuated by shape memory alloy (SMA) wires," in *Proceedings of the ASME 2016 conference on smart materials, adaptive structures and intelligent systems—volume 2: modeling, simulation and control; bio-inspired smart materials and systems; energy harvesting*, Stowe, Vermont, 2016.

[10] S. Quintanar-Guzmán, S. Kannan, A. Aguilera-González, M. A. Olivares-Mendez and H. Voos, "Operational space control of a lightweight robotic arm actuated by shape memory alloy wires: A comparative study," *Journal of Intelligent Material Systems and Structures*, in press.

[11] S. Kannan, S. Quintanar-Guzmán, S. Bezzaoucha, M. A. Olivares-Mendez and H. Voos, "Adaptive control of hysteretic robotic arm in operational space," in *5th International Conference on Mechatronics and Control Engineering ICMCE*, Venice, Italy, 2016.

[12] S. Kannan, S. Bezzaoucha, S. Quintanar-Guzmán, M. A. Olivares-Mendez and V. Holger, "Adaptive Control of Robotic Arms with Hysteretic Joint," in *4th International Conference on Control, Mechatronics and Automation*, Barcelona, Spain, 2016.

[13] S. Kannan, C. Giraud-Audine and E. Patoor, "Application of Laguerre based adaptive predictive control to shape memory alloy (SMA) actuator," *ISA Transactions*, vol. 52, no. 4, pp. 469-479, 2013.

[14] U. A. Asad, P. H. Jaemann, K. Jin, R. Junghyun and C. Maenghyo, "Adaptive control of a shape memory alloy actuator using neural-network feedforward and RISE feedback," *International Journal of Precision Engineering and Manufacturing*, vol. 17, no. 4, pp. 409-418, 2016.

[15] J. Shaw, R. Pan and T. W. Huang, "Adaptive fuzzy sliding mode control of X–Y platform driven by shape memory alloy," *Journal of Intelligent Material Systems and Structures*, vol. 22, no. 16, pp. 1803-1810, 2011.

[16] C. Liang and C. A. Rogers, "One-dimensional thermomechanical constitutive relations for shape memory materials," *Journal of intelligent materials systems and structures*, vol. 1, no. 2, p. 207–234, 1990.

[17] M. H. Elahinia and H. Ashrafiuon, "Nonlinear control of a shape memory alloy actuated manipulator," *Journal of Vibration and Acoustics*, vol. 124, no. 4, p. 566–575, 2002.

[18] M. S. Queiroz, D. M. Dawson, S. P. Nagarkatti and F. Zhang, Lyapunov-Based Control of Mechanical Systems, New York: Springer, 2000.